

Mathematical Modeling of Beating Filaments at Low Reynolds Number

Corey Beck

UC Davis Pure and Applied Math REU 2021

January 2, 2022

Abstract

Microscopic organisms and biological systems at low Reynolds number frequently rely on filament-like appendages known as flagella or cilia for movement. To understand these systems we must model the interactions between filament motion and the surrounding fluid. Differences in fluid characteristics can alter the motion of a singular filament. Other interactions involve coupling forces between multiple filaments. In this model, the filaments are treated as simplified in a two link discrete form, with systems of ordinary differential equations solved numerically to analyze the motion. Through this method we observe and reconfirm known dynamics of motion with a single filament. We also observe varying phase differences between coupled filaments for regimes dependent on coupling strength and initial phase difference.

1 Introduction

In this report we recap the study of beating filaments at low Reynolds number. Reynolds number is the ratio between inertial forces and viscous forces for a given fluid. For a system at low Reynolds number there is no inertial force, so all microorganisms wanting to move must rely entirely on viscous forces at low Reynolds number. One method of motion uses filament-like appendages known as *flagella* or *cilia*. Perhaps most notably, sperm are an organism that operates at low Reynolds number with a single flagella. Organisms that can only move through deformation of their bodies' shape are known as *swimmers*[5].

We wish to study the motion of these systems to better understand the behavior of swimmers at low Reynolds number. In this report, we take an approach by examining isolated filaments with varying structure, a simple approximation of flagella or cilia. Mainly, we will examine the effects of varying types of fluid forces on the motion of a filament at low Reynolds number.

2 Single Filament

To model this motion we will examine a single filament. The motion of this filament can be expanded and compared to that of an organism with a single flagella.

2.1 Continuous Filament

A simple starting case is a single continuous filament fixed but free to rotate on one end, and free to move throughout the fluid on the other. This motion and analysis has been modeled in a previous paper by De Canio, Lauga, and Goldestein[3]. In this example, beating filament dynamics are replicated through the use of a tangential *follower force*. This is a force of constant magnitude applied to the end of a filament pointing tangentially inwards. As described in the paper, this follower force induces a beating motion for low amplitude of oscillation. Following this continuous filament we will discretize the filament for simplicity and better understanding of the mechanics of this system.

2.2 Two Link Filament

A simpler model outlined by De Canio, Lauga, and Goldestein, would be to approximate the continuous model with a filament consisting of two rigid links, connected with “torsion springs” on the joints. This we call the two link model, which is a type of ball and spring model. Each end of a link has a ball that contributes to the viscous drag forces on the system, and the springs model the bending forces in the in the continuous filament.

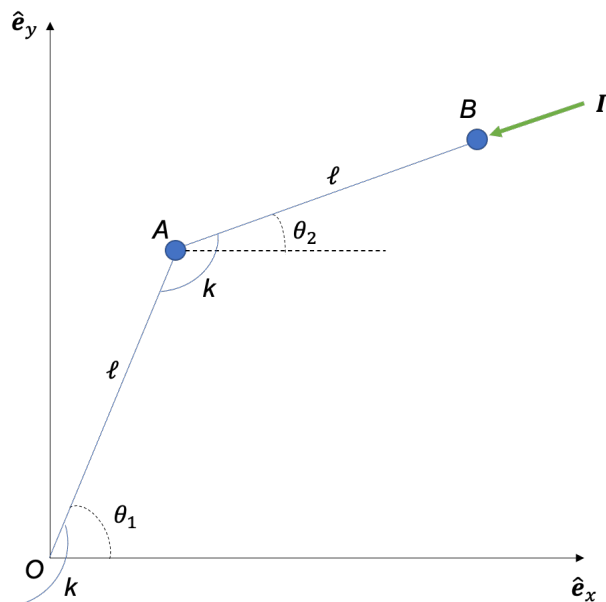


Figure 1: A schematic diagram of the two link filament model.

In this model we have a few physical parameters about the system. Each link has length l , for a total length scale of $2l$, our follower force has strength Γ , each spring has a spring

constant of k , each angle between the base and the links are described as θ_1 and θ_2 , and ζ is the viscous drag coefficient of the balls.

2.2.1 Derivation of Equations of Motion

We would like to create an equation or set of equations that describe the motion of this system. This can be done using the principle of virtual work[3], which is similar to a torque balance.

$$\mathbf{\Gamma} \cdot \delta \mathbf{r}_B + \mathbf{F}_B \cdot \delta \mathbf{r}_B + \mathbf{F}_A \cdot \delta \mathbf{r}_A - k\theta_1 \delta \theta_1 - k(\theta_1 - \theta_2)(\delta \theta_1 - \delta \theta_2) = 0 \quad (1)$$

In this equation the term involving $\mathbf{\Gamma}$ relates to the follower force, the terms with $\mathbf{F}_A, \mathbf{F}_B$ relate to the viscous drag force, and the remaining terms with $\delta \theta_i$'s relate to the restoring force of the springs. The force vectors in the above equation are

$$\begin{aligned} \mathbf{\Gamma} &= -\Gamma \hat{\mathbf{t}} = -\Gamma(\cos \theta_2, \sin \theta_2) \\ \mathbf{F}_A &= -\zeta \mathbf{v}_A \\ \mathbf{F}_B &= -\zeta \mathbf{v}_B \end{aligned}$$

Note in particular we are using a formula for viscous drag coefficient ζ . Using these force vectors we expand the system in terms of θ_i 's and $\delta \theta_i$'s, we obtain the following equations

$$\begin{aligned} \Gamma l \sin(\theta_1 - \theta_2) - 2\zeta l^2 \dot{\theta}_1 - \zeta l^2 \cos(\theta_1 - \theta_2) \dot{\theta}_2 - 2k\theta_1 + k\theta_2 &= 0 \\ -\zeta l^2 \dot{\theta}_2 - \zeta l^2 \cos(\theta_1 - \theta_2) \dot{\theta}_1 + k\theta_1 - k\theta_2 &= 0 \end{aligned} \quad (2)$$

We simplify this system further by nondimensionalizing. We say $\tilde{t} = \frac{k}{\zeta l^2} t$ and define $\Sigma = \frac{\Gamma l}{k}$. We call this value Σ our nondimensional follower force parameter. So with this nondimensionalization our system simplifies to,

$$\Sigma \sin(\theta_1 - \theta_2) - 2\dot{\theta}_1 - \cos(\theta_1 - \theta_2) \dot{\theta}_2 - 2\theta_1 + \theta_2 = 0 \quad (3)$$

$$-\dot{\theta}_2 - \cos(\theta_1 - \theta_2) \dot{\theta}_1 + \theta_1 - \theta_2 = 0 \quad (4)$$

These equations describe the motion of two link filament model. In practice, we will solve these equations numerically in MATLAB with the ode45 or other solvers.

2.2.2 Stability Analysis

We will proceed with a linear stability analysis. This allows us to predict the mechanics on the system for low amplitudes of oscillation. To begin we can take equations 3 and 4 and linearize them about the stable equilibrium $\theta_1 = \theta_2 = 0$. As such, we will approximate $\sin \theta_i \approx \theta_i$ and $\cos \theta_i \approx 1$. With this approximation and the removal of higher order terms we arrive at the following system.

$$\begin{aligned} \Sigma(\theta_1 - \theta_2) - 2\dot{\theta}_1 - \dot{\theta}_2 - 2\theta_1 + \theta_2 &= 0 \\ -\dot{\theta}_2 - \dot{\theta}_1 + \theta_1 - \theta_2 &= 0 \end{aligned} \quad (5)$$

Following this linearization, we can assume a solution to this system takes the form $\theta_i = \hat{\theta}_i e^{\omega t}$. With this our system becomes,

$$\begin{aligned}\Sigma(\hat{\theta}_1 - \hat{\theta}_2) - \omega(2\hat{\theta}_1 + \hat{\theta}_2) - 2\hat{\theta}_1 + \hat{\theta}_2 &= 0 \\ -\omega(\hat{\theta}_1 - \hat{\theta}_2) + \hat{\theta}_1 - \hat{\theta}_2 &= 0\end{aligned}\tag{6}$$

Grouping by $\hat{\theta}_i$ we can represent this system as a matrix and take the determinant, which we will set equal to zero.

$$\omega^2 + 2(3 - \Sigma)\omega + 1 = 0$$

This equation allows us to solve for the ω_{\pm} which can give frequency of filament oscillation in terms of Σ , our single follower force parameter. So,

$$\omega_{\pm} = \Sigma - 3 \pm \sqrt{(\Sigma - 4)(\Sigma - 2)}\tag{7}$$

With this equation for ω_{\pm} we can predict the low amplitude behavior of the system depending on the value of Σ .

- For $0 < \Sigma < 2$, $\text{Re}(\omega_{\pm}) < 0$ and $\text{Im}(\omega_{\pm}) = 0$, so we expect stable decay to the equilibrium $\theta_1 = \theta_2 = 0$.
- For $2 < \Sigma < 3$, $\text{Re}(\omega_{\pm}) < 0$ and $\text{Im}(\omega_{\pm}) \neq 0$, so we expect decaying oscillations to the equilibrium.
- For $\Sigma = 3$, $\text{Re}(\omega_{\pm}) = 0$ and $\text{Im}(\omega_{\pm}) \neq 0$, so we might expect stable, unchanging oscillations. However, as this is a bifurcation point, we do not have a conclusive expectation of the model.
- For $3 < \Sigma < 4$, $\text{Re}(\omega_{\pm}) > 0$ and $\text{Im}(\omega_{\pm}) \neq 0$, so we expect exponentially growing oscillations.
- For $\Sigma > 4$, $\text{Re}(\omega_{\pm}) > 0$ and $\text{Im}(\omega_{\pm}) = 0$, so we expect exponential growth away from equilibrium.

Using MATLAB we confirm that for low amplitude of oscillation the non-linear system of equations describing the two link filament behaves as predicted by the linear stability analysis.

2.2.3 Frequency Extraction

Another topic is to examine the differences between the linear stability analysis and the numerical simulations of the two link model in the viscous case. In this scenario, we will examine the frequency differences between the stability analysis and numerical simulations. The estimated frequencies from the stability analysis come from the following eigenvalues for angular frequency.

$$\omega_{\pm} = \Sigma - 3 \pm \sqrt{(\Sigma - 4)(\Sigma - 2)}$$

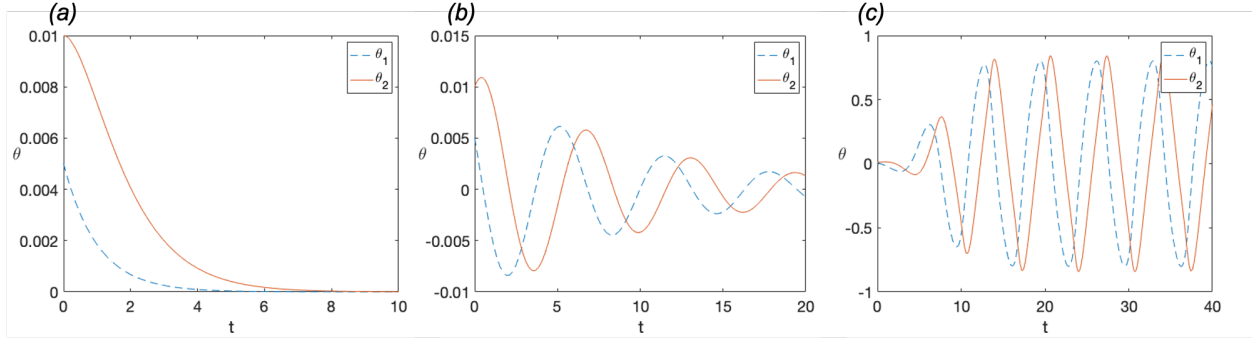


Figure 2: Numerical solutions for a two link model with a small initial deviation from equilibrium. (a) $\Sigma = 2$, (b) $\Sigma = 2.9$, (c) $\Sigma = 3.5$

The analysis predicts oscillations between $2 < \Sigma < 4$ so taking the positive imaginary part of this equation (which correspond to oscillations), we can estimate the frequency of oscillations to be,

$$f_{lin} = \frac{\text{Im}(\omega_+)}{2\pi} = \frac{\sqrt{-(\Sigma - 4)(\Sigma - 2)}}{2\pi}$$

The numerical data was extracted using a Fast Fourier Transform (FFT). This viscous simulation was done in MATLAB by running the simulation for a long enough time to get a time-periodic solution, then taking the largest peak from the frequency spectra. This was then done for a range of values for Σ to get an estimated frequency dependence. Figure 3 displays the relationship between the numerical simulations and the linear stability analysis.

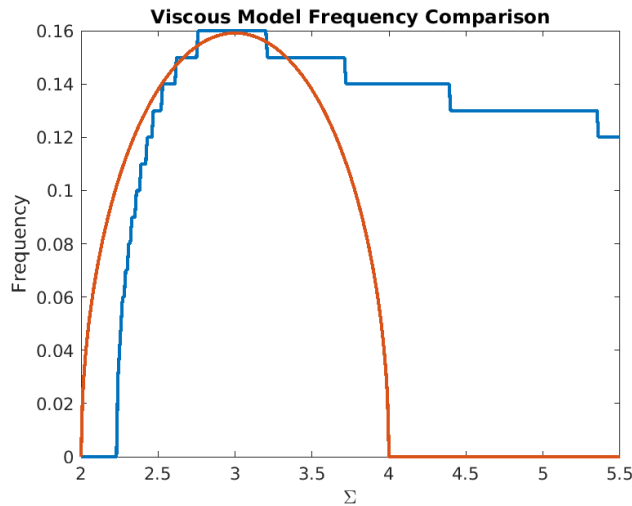


Figure 3: FFT Frequency analysis (blue) compared with stability analysis frequency (red) for varying Σ .

As seen in Figure 3, the values for frequency match closely for values near the bifurcation point ($\Sigma = 3$, where non-decaying oscillations begin) but diverges particularly larger values of

Σ . This is to be expected for large values of Σ , as the stability analysis predicts there would simply be exponential growth away from equilibrium point. This is the case, but larger amplitude (and not particularly sinusoidal) oscillations still occur through observation of simulations for higher values of Σ . The stepwise nature of the FFT analysis is due to a limitation in resolution of frequency provided by the FFT.

2.3 Viscoelastic Model

Another change that can be made to the system is the type of fluid and therefore the fluid force the system experiences. In particular we previously examined the two link filament in a incompressible, viscous fluid. An expansion from this is to a model that contains a *viscoelastic* fluid. In our case, we consider viscoelastic fluids that have a polymer restoring force. This means the fluid can be thought to have “memory” or a location it would return to after deformation.

2.3.1 Maxwell Model

We will use a model known as the Maxwell Model to modify the system of equations we previously had. In this instance, the modification accounts for an additional restoring force σ from polymers in the fluid, ϵ the total strain, ζ_p the viscosity of the polymers, and E the elastic modulus of the polymers. Thus,

$$\frac{\zeta_p}{E} \dot{\boldsymbol{\sigma}} + \boldsymbol{\sigma} = \zeta_p \dot{\boldsymbol{\epsilon}}$$

Setting a new parameter $\lambda = \frac{\zeta_p}{E}$ and replacing the right hand side with our viscous force from earlier we get the following new equation for motion,

$$\lambda \dot{\boldsymbol{\sigma}} + \boldsymbol{\sigma} = -\zeta \mathbf{v} \quad (8)$$

where ζ is the viscosity of the fluid. Introducing this for each ball on the two link filament we can obtain the new system of equations.

$$\boldsymbol{\Gamma} \cdot \delta \mathbf{r}_B + \boldsymbol{\sigma}_B \cdot \delta \mathbf{r}_B + \boldsymbol{\sigma}_A \cdot \delta \mathbf{r}_A - k\theta_1 \delta\theta_1 - k(\theta_1 - \theta_2)(\delta\theta_1 - \delta\theta_2) = 0 \quad (9)$$

$$\lambda \dot{\boldsymbol{\sigma}}_A + \boldsymbol{\sigma}_A = -\zeta \mathbf{v}_A$$

$$\lambda \dot{\boldsymbol{\sigma}}_B + \boldsymbol{\sigma}_B = -\zeta \mathbf{v}_B$$

Expanding this system we end up with 6 equations, two differential equations and 2 constraint equations. This can again be solved numerically in MATLAB.

$$0 = -\Gamma l \sin(\theta_2 - \theta_1) + l [-(\sigma_{A_x} + \sigma_{B_x}) \sin \theta_1 + (\sigma_{A_y} + \sigma_{B_y}) \cos \theta_1] + k(\theta_2 - 2\theta_1) \quad (10)$$

$$0 = l [-\sigma_{B_x} \sin \theta_2 + \sigma_{B_y} \cos \theta_2] - k(\theta_2 - \theta_1)$$

$$\lambda \dot{\sigma}_{A_x} + \sigma_{A_x} = \zeta l \dot{\theta}_1 \sin \theta_1$$

$$\lambda \dot{\sigma}_{A_y} + \sigma_{A_y} = -\zeta l \dot{\theta}_1 \cos \theta_1$$

$$\lambda \dot{\sigma}_{B_x} + \sigma_{B_x} = \zeta l (\dot{\theta}_1 \sin \theta_1 + \dot{\theta}_2 \sin \theta_2)$$

$$\lambda \dot{\sigma}_{B_y} + \sigma_{B_y} = -\zeta l (\dot{\theta}_1 \cos \theta_1 + \dot{\theta}_2 \cos \theta_2)$$

2.3.2 Nondimensionalization

Similarly to the viscous case we nondimensionalize this system to leave as few parameters as possible. First we scale our time factor by $T = \frac{\zeta l^2}{k}$. We would like to vary λ freely as the parameter corresponding to the polymers so we define a new parameter as the ratio of polymer strength to viscous strength to be $\Lambda = \frac{k\lambda}{\zeta l^2}$ along with our familiar follower force parameter $\Sigma = \frac{\Gamma l}{k}$. This gives us the following nondimensionalized system.

$$\begin{aligned}
0 &= -\Sigma \sin(\theta_2 - \theta_1) - (\sigma_{A_x} + \sigma_{B_x}) \sin \theta_1 + (\sigma_{A_y} + \sigma_{B_y}) \cos \theta_1 + \theta_2 - 2\theta_1 & (11) \\
0 &= -\sigma_{B_x} \sin \theta_2 + \sigma_{B_y} \cos \theta_2 - \theta_2 + \theta_1 \\
\Lambda \dot{\sigma}_{A_x} + \sigma_{A_x} &= \dot{\theta}_1 \sin \theta_1 \\
\Lambda \dot{\sigma}_{A_y} + \sigma_{A_y} &= -\dot{\theta}_1 \cos \theta_1 \\
\Lambda \dot{\sigma}_{B_x} + \sigma_{B_x} &= (\dot{\theta}_1 \sin \theta_1 + \dot{\theta}_2 \sin \theta_2) \\
\Lambda \dot{\sigma}_{B_y} + \sigma_{B_y} &= -(\dot{\theta}_1 \cos \theta_1 + \dot{\theta}_2 \cos \theta_2)
\end{aligned}$$

2.3.3 Stability Analysis

Again similarly to the viscous case we can linearize the system of equations, which in turn reduces down to 4 equations.

$$\begin{aligned}
0 &= \Sigma(\theta_1 - \theta_2) + (\sigma_{A_y} + \sigma_{B_y}) + (\theta_1 - 2\theta_2) & (12) \\
0 &= \sigma_{B_y} - (\theta_2 - \theta_1) \\
\Lambda \dot{\sigma}_{A_y} + \sigma_{A_y} &= -\dot{\theta}_1 \\
\Lambda \dot{\sigma}_{B_y} + \sigma_{B_y} &= -(\dot{\theta}_1 + \dot{\theta}_2)
\end{aligned}$$

Repeating the process of the viscous system we find the following equation for ω_{\pm} near the equilibrium point of 0.

$$\omega_{\pm} = \frac{\Sigma - \Lambda - 3 \pm \sqrt{(\Sigma - 4)(\Sigma - 2)}}{-2\Sigma\Lambda + \Lambda^2 + 6\Lambda + 1}. \quad (13)$$

Note that when $\Lambda = 0$, ω_{\pm} is the same as the viscous model. One method of visualizing the behavior of the model is with contour plots. The two in Figure 4 represent the positive root of ω_{\pm} which then display information relating to both the exponential growth/decay of the system, as well as the oscillatory nature of the system. Following along the bottom axis of $\Lambda = 0$ we recover the viscous model. A particularly interesting note about this system is that as Λ increases, the region for exponential decay shifts to higher values of Σ .

An unfortunate result of the Maxwell Model was the inability to simulate large values of Λ . The non-linear DAE system of equations continued to run into a singularity when $\Lambda > 1$ regardless of the solver used in MATLAB. As such, most results occurred with low polymer forces close to the viscous model. However, other group members of this project proceeded with a different model and were able to achieve more successful results for higher viscoelastic forces.

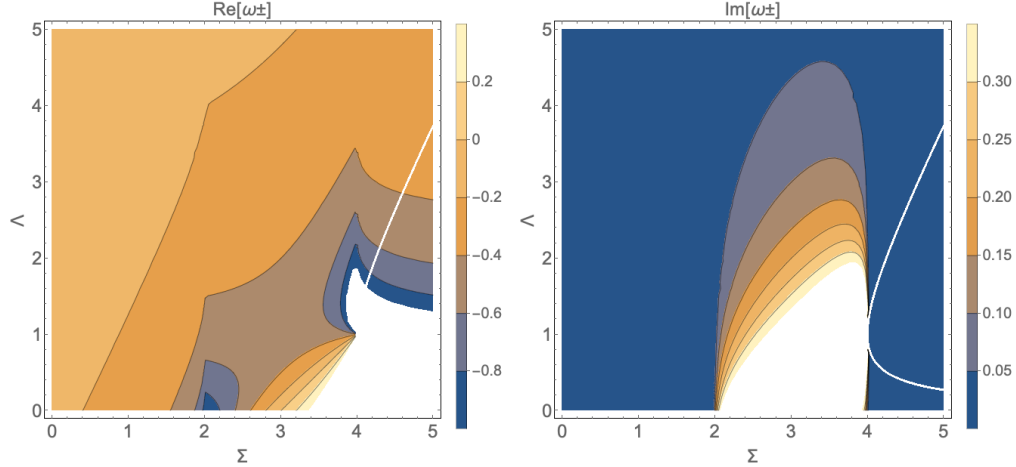


Figure 4: Pertaining to the viscoelastic two-link filament model, the imaginary part of ω_{\pm} corresponds to the frequency of oscillation, whereas the real part of ω_{\pm} corresponds to exponential growth or decay, from our stability analysis.

3 Coupled Filaments

3.1 Model

The model for this system is created from two discrete filaments. Unlike the two link viscous model, we cannot as easily nondimensionalize the system, so we will have many parameters. Similar to the two link viscous model we apply an equal tangential follower force to each filament with strength Γ . For our size parameters, the balls have diameter ϵ , the filaments are separated by the distance d , and each link of the filament has length l , where $\epsilon < d < 2l$. Much of this setup is a discretization of a similar model continuous in a paper by Man and Kanso[4]. A sketch of this model is outlined in Figure 5.

3.2 Derivation

The equation of motion for this system can be derived through a torque balance. We equate the torques of the follower forces and the coupled fluid forces with the restoring force of the springs.

$$\mathbf{\Gamma}_1 \cdot \delta \mathbf{r}_{12} + \mathbf{\Gamma}_2 \cdot \delta \mathbf{r}_{22} + \mathbf{F} \cdot \delta \mathbf{r} = \mathbf{F}_{rest} \cdot \delta \boldsymbol{\theta} \quad (14)$$

In this scenario, $\mathbf{\Gamma}_1, \mathbf{\Gamma}_2$ are the follower forces, \mathbf{F} is the force corresponding to the fluid and the coupling motion and \mathbf{F}_{rest} is shorthand combination of all of the restoring forces from the spring-like joints. To find the fluid force we will use a solution to Stokes's Equations where initially each ball is treated as a point force. The intuition behind this system is that movement of a ball (a point of our filament) in a fluid will affect all of the surrounding fluid. In this scenario the fluid is an incompressible Newtonian fluid with viscosity μ . As such, a point force in a fluid will induce a velocity field. Comparing all these forces and velocity fields we can create a system that relates forces and movement of the filaments. We can

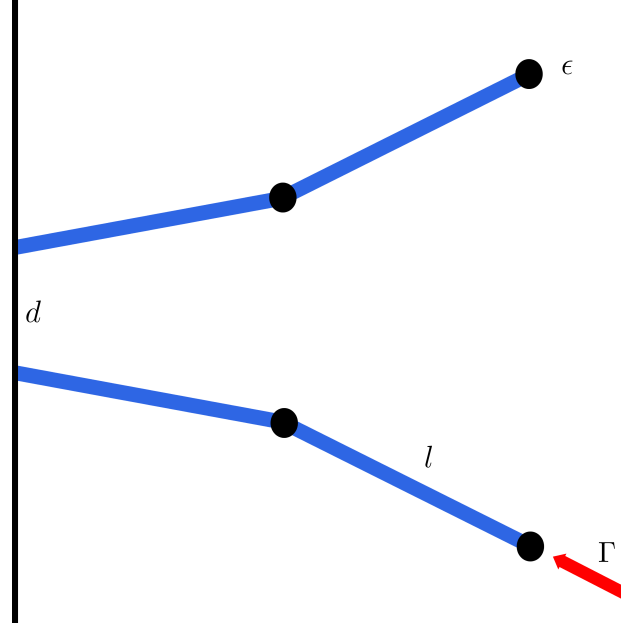


Figure 5: A diagram of the model to be used for coupled motion analysis.

begin by solving the Stokes equations.

$$\mu \Delta \mathbf{U} - \nabla p + \mathbf{F} \delta(x - x_0) = 0 \quad (15)$$

$$\nabla \cdot \mathbf{U} = 0 \quad (16)$$

Using a method known as the Method of Regularized Stokeslets, we obtain a regularized solution relating the fluid velocity at a point and the force from another point[1, 2].

$$u_i = \frac{1}{8\pi\mu} S_{ij}^\epsilon F_j \quad (17)$$

$$S_{ij}^\epsilon(\mathbf{x}, \mathbf{x}_0) = \delta_{ij} \frac{r^2 + 2\epsilon^2}{(r^2 + \epsilon^2)^{3/2}} + \frac{(x_i - (x_0)_i)(x_j - (x_0)_j)}{(r^2 + \epsilon^2)^{3/2}} \quad (18)$$

In these equations u_i represents the velocity of one ball in our diagram, and F_j is the force a different ball exerts on it. The term S_{ij} is called a *Stokeslet* and r is the distance between the two points \mathbf{x} and \mathbf{x}_0 the Stokeslet is describing in the fluid. We can represent this as

$$\mathbf{U} = M \mathbf{F}$$

where U is the vector of velocities, F is the vector of forces and M is the matrix relating the two with Stokeslets. As the Stokeslet matrix has entries on the diagonal, it will always be invertible so we write

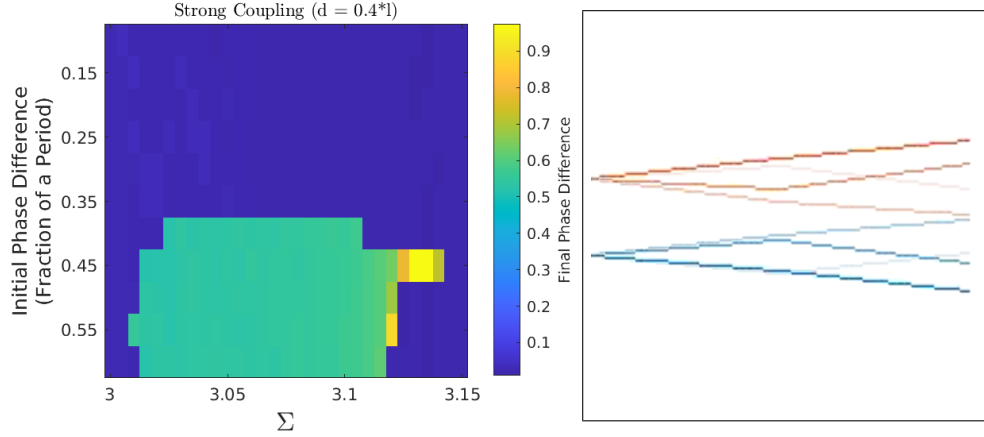
$$M^{-1} \mathbf{U} = \mathbf{F}$$

We can then describe U in terms of θ_i 's and substitute into our torque balance. This then gives a system that can be solved numerically in MATLAB.

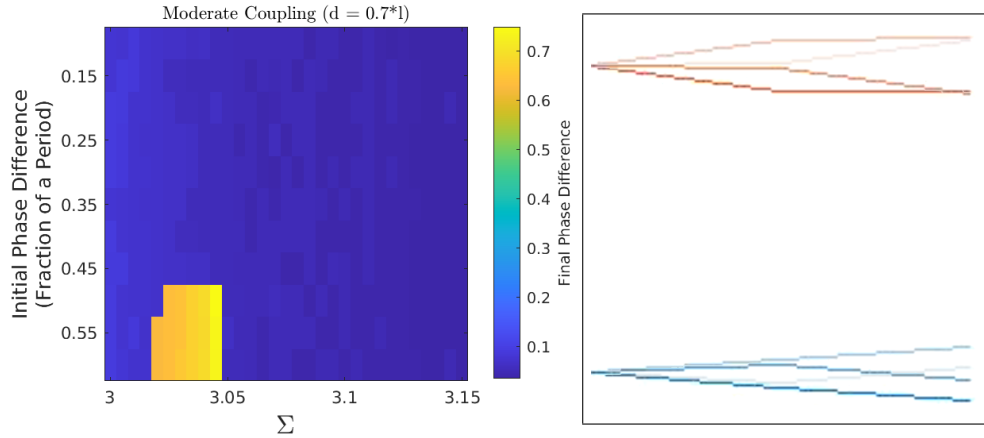
Our main focus in the final motion is the phenomenon known as phase locking. We expect the filaments to have similar oscillatory motion and a constant phase difference in the final state. We anticipate seeing filaments moving in parallel, but could also observe other motion. To determine a phase difference we begin the simulation with arbitrary phase differences between the two filaments and run the simulation until it reaches a steady state. Then a final phase difference can be calculated between the two filaments. For a systematic approach we choose 3 different couplings strengths. These are determined by the separation distance of the filaments. We use $d = 0.4l$ for strong coupling, $d = 0.7l$ for moderate coupling, and $d = 1.6l$ for weak coupling. For each particular strength of coupling we vary both the initial phase difference of the filaments and Σ , our nondimensionalized follower force parameter. We use Σ as defined earlier in the viscous case in order to observe similar oscillation amplitude and behavior for the viscous case. As such, many of our oscillations take place where Σ is slightly greater than 3, which is where our smallest amplitude of oscillation takes place.

3.3 Results

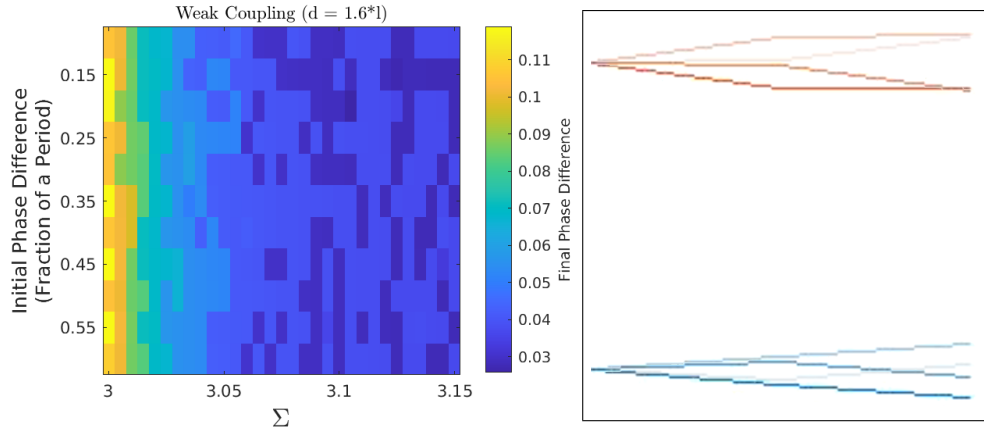
Figure 6 displays the relationships between the initial phase difference and follower force strength for each strength of coupling. For strong coupling we see zones where the filaments phase lock in parallel and also anti-parallel. For the moderate coupling we see a majority zone of parallel phase locking, but also a small region of non-trivial phase locking. This region has about a 0.6 period difference between the filaments. So they are not anti-parallel, but some other fraction out of phase. Finally for weak coupling we see a very small section of very small phase difference. This occurs for tiny amplitudes of oscillation and appears to be a small lag behind of one filament from the other. These non-trivial components of phase locking result from this method of coupling between filaments, specifically at low amplitude.



(a) Strong Coupling ($d = 0.4l$)



(b) Moderate Coupling ($d = 0.7l$)



(c) Weak Coupling ($d = 1.6l$)

Figure 6: Left: Final phase difference dependent on initial phase difference and nondimensional follower force Σ , for strong ($d = 0.4l$), moderate ($d = 0.7l$), and weak ($d = 1.6l$) coupling. Right: Simulated filament visualizations for each non-trivial phase locking example. Time is indicated by opacity of filament.

4 Conclusion

We have summarized known research and laid the groundwork for future research of beating filaments. Some future questions arise from this model. Examples of these may be, higher link number filaments, loaded filaments[3], continuous filament coupling[4], uneven follower forces for coupling, and more than two filaments for coupling. These questions are interesting extensions of the groundwork laid by the two link, two filament, coupled model outlined in this report.

5 Acknowledgements

Thank you to mentors Bob Guy, Becca Thomases, and Kathryn Link. Thanks as well to research group members Sophia Nelson and Michaela Rapier for their assistance with this project. This research was conducted as part of the 2021 UC Davis Pure and Applied Math REU, supported by the National Science Foundation under grant no. DMS 1950928.

References

- [1] Ricardo Cortez. The method of regularized stokeslets. *SIAM Journal on Scientific Computing*, 23(4):1204–1225, 2001.
- [2] Ricardo Cortez, Lisa Fauci, and Alexei Medovikov. The method of regularized stokeslets in three dimensions: Analysis, validation, and application to helical swimming. *Physics of Fluids*, 17(3):031504, 2005.
- [3] Gabriele De Canio, Eric Lauga, and Raymond E. Goldstein. Spontaneous oscillations of elastic filaments induced by molecular motors. *Journal of The Royal Society Interface*, 14(136), 2017.
- [4] Yi Man and Eva Kanso. Multisynchrony in active microfilaments. *Physical Review Letters*, 125(14), Oct 2020.
- [5] Edward M. Purcell. Life at low reynolds number. *AIP Conference Proceedings*, 1976.